# Synthesis and Exciton Optical Activity of $D_3$-Cryptophanes†

**Josette Canceill,‡ André Collet,*‡ Giovanni Gottarelli,§ and Paolo Palmieri‖**

*Contribution from the Collège de France, Chimie des Interactions Moléculaires, 75231 Paris Cedex 05, France, Dipartimento di Chimica Organica, Università di Bologna, 40127 Bologna, Italy, and Dipartimento di Chimica Fisica ed Inorganica, Università di Bologna, 40136 Bologna, Italy.* *Received February 20, 1987*

**Abstract:** Six optically active $D_3$-cryptophanes (**1–6**) have been synthesized and their absolute configurations established unambiguously. In order to explain their circular dichroism (CD) spectra, a simple theoretical model, based on the Kuhn–Kirkwood exciton mechanism, has been developed for the coupling of six equivalent oscillators in a $D_3$ molecular point group. The model predicts for each $B_{2u}$ and $B_{1u}$ benzene transition the presence of three CD components, one ($A_2$) being polarized along the $C_3$ axis and two (E) in the plane containing the $C_2$ axes. The two E components have opposite signs and different intensities, the stronger having sign opposite to the $A_2$ transition. The splitting between the E states in each band system is dependent on the twist angle ($2\gamma$) between the upper and the lower caps of the molecule. For $2\gamma = 60°$ (staggered conformation), this splitting is estimated to be very small, compared to the corresponding $E - A_2$ energy difference, and the E components are never resolved in the theoretical plotted spectra for any realistic bandwidth. For $2\gamma = 0°$ (eclipsed conformation), the calculated splitting of the E states is large enough to become apparent in plotted spectra for the $B_{1u}$ system. When a staggered conformation is assumed, the experimental CD spectra of cryptophanes **1–6** have been, in most cases, satisfactorily interpreted in terms of the model, with the polarization direction of the transitions set in accordance to the spectroscopic moment theory by using the rules previously established for $C_3$-cyclotriveratrylenes. In some cases, the energy sequence of the E states for the $B_{2u}$ system is not in agreement with the predictions, probably due to the failure of the point–dipole approximation to determine the exact sequence of almost degenerate states. The results of this study point out the importance of the coupled-oscillator model in explaining the CD spectra of complex molecules containing more than three oscillators.

Of the theories and empirical rules that aim at correlating optical rotation or circular dichroism (CD) data with molecular structure and handedness, the Kuhn–Kirkwood coupled-oscillator model[1] is particularly attractive and useful for several reasons: (i) It is based on physical concepts that are simple and can easily be applied by *nonspecialists*. (ii) Its scope is well-defined and limited to molecules containing a few chromophoric units interacting through their electric transition dipoles induced by a radiation field. (iii) It normally gives rise to strong and characteristic Cotton effects (exciton optical activity) whose signs and magnitude are, in many instances, unambiguously predictable, thus leading to safe configurational or conformational assignments.

With the pioneering work by Mason in the 1960s[2] and with the development of molecular spectroscopy and the subsequent better knowledge of the polarization direction of the electronic transitions in a variety of chromophores, the model has become increasingly used by organic as well as inorganic chemists, as illustrated by the large number of applications recently quoted by Harada and Nakanishi.[3]

Until now, the Kuhn–Kirkwood mechanism has mainly been observed and used for stereochemical applications, in the case of molecules containing two coupled oscillators, for instance diol dibenzoates,[4] *trans*-stilbene oxide,[5] biaryl derivatives,[6,7] etc. There are several studies dealing with compounds containing three oscillators in the field of coordination metal complexes,[8] and very few among organic molecules.[9-12] To our knowledge, apart from helical polymers,[13] the theory has not yet been extended to systems containing more than three coupled chromophores, and its usefulness and limitations in such cases have therefore not been established.

In this paper, we deal with the problem of the exciton optical activity of molecules with a $D_3$ array of *six* equivalent oscillators; such a situation occurs in the cryptophanes[14] **1–6**, which therefore provide a relevant set of experimental models for testing the theory in this case. Originally, these compounds were designed to achieve selective complexation of lipophilic guest molecules (halogenomethanes),[15-18] and the possibility of using the CD technique as a tool for the complexation studies seemed worth considering. The chiral cryptophanes **1–6** are made of two identical (homochiral) $C_3$-cyclotribenzylene caps linked to one another by short bridges of various structures (i.e. Z in Chart I); their geometry is known

**Chart I.** Syntheses and Configurational Assignments

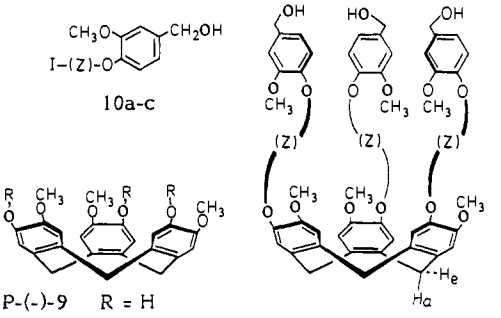


Z = a $-CH_2-CH_2-$; b $-CH_2-CH_2-CH_2-$; c $-CH_2-C\equiv C-CH_2-$

P-(-)-9 + 10a → (+)-11a → (-)-1 → (-)-4 → (-)-5, (-)-6; 10b → (+)-11b → (-)-2 + 7; 10c → (+)-11c → (-)-3 + 8

† Dedicated to S. F. Mason on the occasion of his 65th birthday.
‡ Collège de France, E.R. CNRS No. 285.
§ Dipartimento di Chimica Organica.
‖ Dipartimento di Chimica Fisica ed Inorganica.

(1) Kuhn, W. *Trans. Faraday Soc.* **1930**, *26*, 293. Kirkwood, J. G. *J. Chem. Phys.* **1937**, *5*, 479–491.
(2) Mason, S. F. *Q. Rev., Chem. Soc.* **1963**, *17*, 20–66.
(3) Harada, N.; Nakanishi, K. *Circular Dichroism Spectroscopy – Exciton Coupling in Organic Stereochemistry*; University Science Books: New York, 1983.
(4) Harada, N.; Nakanishi, K. *Acc. Chem. Res.* **1972**, *5*, 257–263.
(5) Gottarelli, G.; Mason, S. F.; Torre, G. *J. Chem. Soc. B* **1970**, 1349–1353.
(6) Mason, S. F.; Seal, R. H.; Roberts, D. R. *Tetrahedron* **1974**, *30*, 1671–1682.
(7) Seno, K.; Hagishita, S.; Sato, T.; Kuriyama, K. *J. Chem. Soc., Perkin Trans. 1* **1984**, 2013–2022.
(8) Mason, S. F. *Molecular Optical Activity and the Chiral Discriminations*; Cambridge University: Cambridge, 1982; Chapter 6, pp 83–87 and references therein.

0002-7863/87/1509-6454$01.50/0 

from X-rays[17-19] or can be predicted relatively accurately from molecular models. Furthermore, the optical activity of the $C_3$-cyclotribenzylene units has been investigated in detail and successfully analyzed in light of the coupled-oscillator mechanism, extended to three chromophores.[10] During these studies, accurate information on the polarization direction of the $B_{2u}$ and $B_{1u}$ transitions as a function of the substitution pattern of the benzene rings has been obtained. These results will prove useful in the context of the present study.

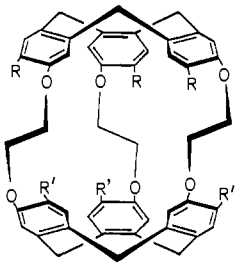

(-)-1 R = R' = $OCH_3$
(-)-4 R = R' = OH
(-)-5 R = R' = $OCOCH_3$
(-)-6 R = R' = $OCH_2CO_2CH_3$
(-)-13 R = $OCH_3$ R' = H

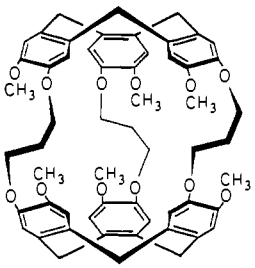

(-)-2

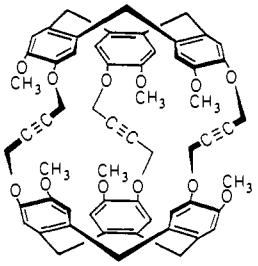

(-)-3

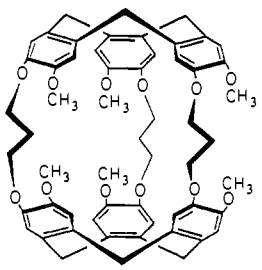

7

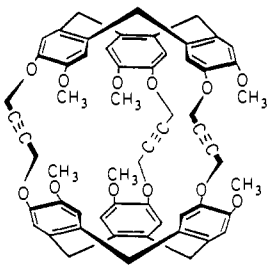

8

This paper is divided into three main sections. The first one deals with syntheses and absolute configuration assignments and presents the CD spectra of the chiral cryptophanes **1–6**. In the second part, the theoretical treatment for six coupled oscillators in a $D_3$ arrangement is presented. In the third part (Discussion), the theoretical predictions and the experimental CD spectra of **1–6** are compared. We conclude that the coupled-oscillator approach, in its simple point-dipole approximation form, works reasonably well for $D_3$ systems containing six chromophores.

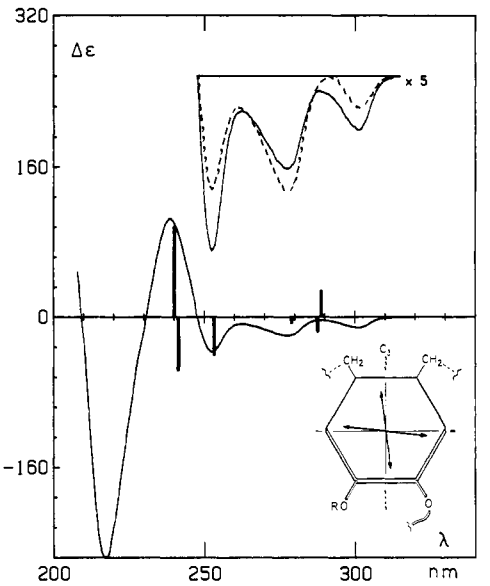


**Figure 1.** CD spectra of (-)-**1**: in dioxane, empty cage (solid line); in dioxane/chloroform (8:2), chloroform complex (dotted line). The bars represent the calculated components of the $B_{2u}$ and $B_{1u}$ transitions, for $\theta = -1.5°$ and $\theta' = +2.5°$ (the corresponding polarization directions are sketched in the inset, the angles being exaggerated for clarity).

### Syntheses, Absolute Configurations, and Chiroptical Data

The absolute configurations of the (-)-cryptophanes **1–6** (displayed on the stereoformulas) were established on the basis of the synthetic sequence summarized in Chart I; **1** and **2** (cryptophanes A[20] and E,[18] respectively) have already been described, but no details of their synthesis have been provided. In a first step, the known[10,11] enantiomerically pure *P*-(-)-cyclotriguaiacylene **9**, on alkylation by the iodides **10a–c**, furnished the cryptophane precursors *M*-(+)-**11a–c**, which in turn when submitted to acidic conditions ($HCO_2H$, 50–90 °C; or $HClO_4$ in $CH_3CO_2H$, 20 °C) afforded the desired compounds (-)-**1–3**. The intramolecular cyclization of the vanillyl alcohol residues of (+)-**11a** was stereospecific, giving (-)-**1** as the only isolable product in 70–80% yield. In contrast, (+)-**11b**, under the same conditions, gave a mixture of (-)-**2** (27%) and its meso (achiral) isomer **7** (50%); likewise, (+)-**11c** yielded (-)-**3** (30%) and **8** (14%). The structures of the new compounds **7** and **8** (cryptophanes G and H, respectively) were established by NMR and FABMS.

The new cryptophanes (-)-**4–6** were synthesized from (-)-**1**. The key step was to cleave the six methyl ethers of **1** without affecting the three ethylenedioxy bridges. This was satisfactorily achieved by using lithium diphenylphosphide (THF, 20 °C), a very mild and selective demethylation reagent;[21] in this way, (-)-**4** could be secured in 60% yield. This compound, on acetylation (acetic anhydride/pyridine), gave the hexaacetate (-)-**5** and, on reaction with methyl bromoacetate ($Cs_2CO_3$ in DMF), eventually furnished (-)-**6**.

The optical rotations of the cryptophanes **1–6** obtained by this route are reported in Table I. For the clarity of the discussion, all the structural formulas and chiroptical data throughout this

(9) Reference 3, pp 203–212. For the coupling of several *different* chromophoric groups see also: Wiesler, W. T.; Waskez, J. T.; Nakanishi, K. *J. Am. Chem. Soc.* **1986**, *108*, 6811–6813.
(10) Canceill, J.; Collet, A.; Gabard, J.; Gottarelli, G.; Spada, G. P. *J. Am. Chem. Soc.* **1985**, *107*, 1299–1308.
(11) Canceill, J.; Collet, A.; Gottarelli, G. *J. Am. Chem. Soc.* **1984**, *106*, 5997–6003.
(12) Canceill, J.; Collet, A. *Nouv. J. Chim.* **1986**, *10*, 17–23.
(13) Reference 8, pp 88–96 and references therein.
(14) Canceill, J.; Lacombe, L.; Collet, A. *J. Am. Chem. Soc.* **1985**, *107*, 6993–6996.
(15) Canceill, J.; Lacombe, L.; Collet, A. *C. R. Acad. Sci., Ser. 2* **1984**, *298*, 39–42.
(16) Canceill, J.; Cesario, M.; Collet, A.; Guilhem, J.; Pascard, C. *J. Chem. Soc., Chem. Commun.* **1985**, 361–363.
(17) Canceill, J.; Cesario, M.; Collet, A.; Guilhem, J.; Riche, C.; Pascard, C. *J. Chem. Soc., Chem. Commun.* **1986**, 339–341.
(18) Canceill, J.; Lacombe, L.; Collet, A. *J. Am. Chem. Soc.* **1986**, *108*, 4320–4322. Canceill, J.; Lacombe, L.; Collet, A. *C. R. Acad. Sci., Ser. 2* **1987**, *304*, 815–818.
(19) The crystal structure of cryptophane E will be published in a forthcoming paper. We thank M. Cesario, J. Guilhem, and C. Pascard (CNRS, Gif-sur-Yvette) for providing us with all the necessary structural data prior to publication.
(20) Gabard, J.; Collet, A. *J. Chem. Soc., Chem. Commun.* **1981**, 1137–1139.
(21) (a) Ireland, R. E.; Walba, D. M. *Org. Synth.* **1977**, *56*, 44–48. (b) Vedejs, E.; Fuchs, P. L. *J. Am. Chem. Soc.* **1973**, *95*, 822–825.
(22) Collet, A. In *Inclusion Compounds*; Atwood, J. L., Ed.; Academic: London, 1984; Vol. II, Chapter 4.

Table I. Specific Rotations of Cryptophanes 1–6

| compd | solvent | concn, g/100 mL | $[\alpha]_\lambda^{25}$, deg | | | | |
|---|---|---|---|---|---|---|---|
| | | | 589 | 578 | 546 | 436 | 365 |
| (−)-**1** | $CHCl_3$ | 0.18–0.30 | −253 | −265 | −306 | −574 | −1069 |
| (−)-**2**[a] | $CHCl_3$ | 0.9 | −49 | −51 | −60 | −110 | |
| (−)-**3**[a] | $CHCl_3$ | 0.44 | −201 | −211 | −242 | −442 | −782 |
| (−)-**4** | DMF | 0.21 | −172 | −181 | −209 | −406 | −799 |
| (−)-**5** | $CHCl_3$ | 0.24 | −24 | −25 | −28 | −58 | −133 |
| (−)-**6** | $CHCl_3$ | 0.39 | −116 | −122 | −140 | −269 | −530 |

[a] Measured on the enantiomer.

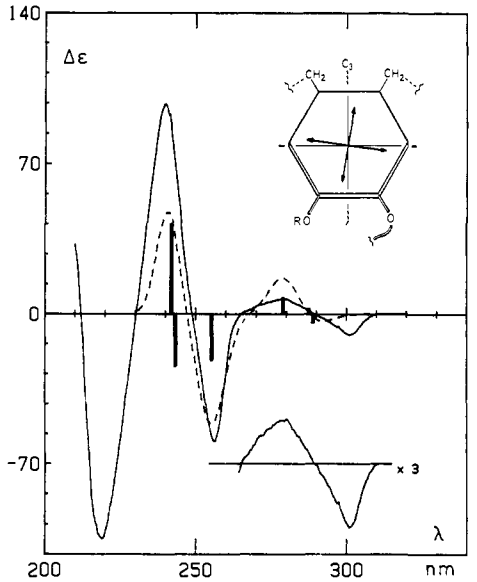


Figure 2. CD spectrum of (−)-**2** in dioxane. The theoretical spectrum (bars and dotted line) was calculated with $\theta = +1.5°$ and $\theta' = +4°$.

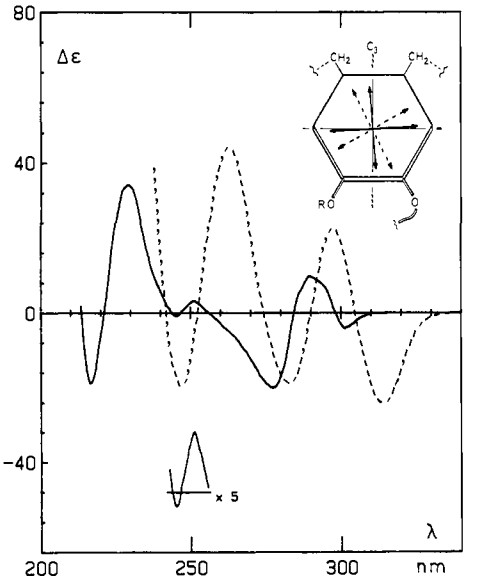


Figure 4. CD spectra of (−)-**4** in methanol (solid line) and in methanol containing sodium methoxide (0.5 M) (dotted line).

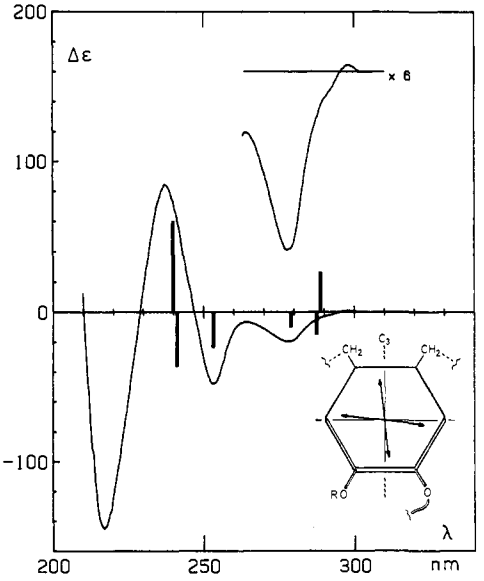


Figure 3. CD spectrum of (−)-**3** in dioxane with the $B_{2u}$ region enlarged, showing the three components; calculated components (bars) with $\theta = -2°$ and $\theta' = +2°$.

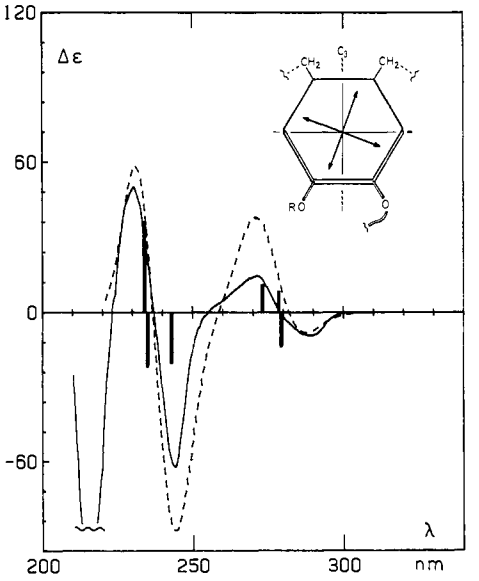


Figure 5. CD spectrum of (−)-**5** in dioxane; theoretical spectrum (bars and dotted line) calculated with $\theta = \theta' = +15°$.

paper (except the Experimental Section) refer to the (−)-enantiomers, although in some cases only the (+)-cryptophane was available.

So far, our attempts to measure the ee of these cryptophanes by $^1H$ NMR in the presence of a chiral LSR ($Eu(dcm)_3$) have failed; we have, however, some indirect evidence that these compounds are probably not far from being enantiomerically pure. First, the precursors **11a–c** were prepared and isolated under very mild conditions ($T \leq 20$ °C during the reaction and subsequent workup) in order to avoid racemization via crown inversion;[10–12] hence, their ee should be the same as that of **9**, i.e. ≥95%. Then, although there was a risk that some racemization would occur during the conversion of the precursors to the cryptophanes, especially when this reaction was effected at 50–90 °C, experiments with (+)-**11a** showed that the temperature at which the cyclization was performed had only a moderate influence on the rotation of **1** (isolated by TLC). Similar observations have been reported for the preparation of cryptophane C (**13**).[14] From the racemization rates at several temperatures the activation parameters for crown inversion in **11a** were obtained: $\Delta H^\ddagger = 25.8 \pm 0.5$ kcal/mol, $\Delta S^\ddagger = -3 \pm 1$ cal·mol$^{-1}$·K$^{-1}$. The racemization half-

Table II. CD and UV Data for Cryptophanes (−)-**1**–**6**

| | (−)-1 (dioxane) | | (−)-2 (dioxane) | | (−)-3 (dioxane) | | (−)-4 (OH) (methanol) | | (−)-4 (ONa) (methanol/ MeONa) | | (−)-5 (dioxane) | | (−)-6 (dioxane) | |
|---|---|---|---|---|---|---|---|---|---|---|---|---|---|---|
| | λ | Δε | λ | Δε | λ | Δε | λ | Δε | λ | Δε | λ | Δε | λ | Δε |
| | 217 | −255 | 219 | −105 | 217 | −145 | 229.5 | +34 | 230.5 | +89 | 215 | −104 | 218.5 | −201 |
| $B_{2u}$ | 238.5 | +104 | 240 | +98 | 237 | +84 | 245.5 | −0.7 | 247 | −22 | 230.5 | +50 | 237.5 | +90 |
| | 252.5 | −37 | 256 | −60 | 253.5 | −48 | 251.5 | +3.3 | 263 | +50 | 244.5 | −62 | 251 | −38 |
| | 277.5 | −24.5 | 280 | +6.9 | 278 | −19.8 | 277.5 | −20 | 283 | −21 | 271.5 | +14.6 | | |
| $B_{1u}$ | | | | | 292 sh | −1.7 | 289.5 | +9.9 | 297.5 | +25 | | | | |
| | 301.5 | −11.4 | 301 | −9.8 | 298 | +0.7 | 301.5 | −4.2 | 315 | −24.5 | 299 | −37 | 297 | −16.9 |

| (−)-1 (dioxane) | | (−)-2 (dioxane) | | (−)-3 (dioxane) | | (−)-4 (OH) (methanol) | | (−)-4 (ONa) (methanol/ MeONa) | | (−)-5 (dioxane) | | (−)-6 (dioxane) | |
|---|---|---|---|---|---|---|---|---|---|---|---|---|---|
| λ | ε | λ | ε | λ | ε | λ | ε | λ | ε | λ | ε | λ | ε |
| 207 | (115 000) | 205 | (130 000) | 208 | (100 000) | 199 | (120 000) | 204 | (170 000) | | | 207 | (56 000) |
| 231 | 47 000 | 235 | 60 100 | 234 | 44 000 | 228 sh | 38 000 | 234 sh | 34 000 | 224 sh | 51 700 | 229 | 46 000 |
| 241 i | 31 200 | 247 i | 27 000 | 242 i | 28 000 | | | 250 i | 20 400 | 236 i | 31 700 | | |
| 228 | 14 000 | 281 sh | 16 900 | 280 i | 10 900 | | | | | | | | |
| 293 sh | 13 900 | 287 sh | 18 800 | 292 | 13 300 | 288 | 12 900 | 299 | 13 600 | 284 | 10 000 | 286 | 11 850 |
| | | 292 | 19 000 | | | | | | | | | 291 sh | 11 500 |
| | | 298 | 18 500 | | | | | | | | | | |

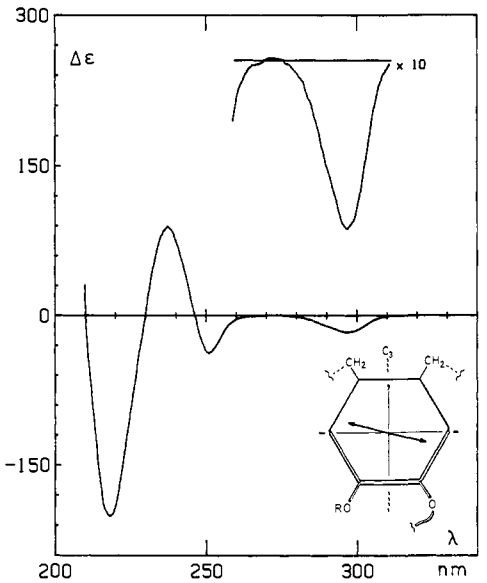


**Figure 6.** CD spectrum of (−)-**6** in dioxane, with the $B_{2u}$ region enlarged. Only the direction of the $B_{1u}$ transition dipole (insert) could be determined.

times were ca. 48 days, 5 h, and 10 min at 20, 50, and 90 °C, respectively. The fact that the rotation of **1** was hardly affected by the reaction temperature therefore indicates that, compared to the crown inversion rate, the intramolecular trimerization of the veratryl ends in the precursor is fast.

**Spectral Data.** The CD spectra of the (−)-cryptophanes **1**–**6** are reported in Figures 1–6, and relevant UV and CD data are assembled in Table II. The effect of complexation was studied in the cases of **1**–**3** as a possible way of detecting conformational changes that might be induced in the cryptophanes on guest inclusion. To this end, the empty hosts were prepared by dissolving the crystalline cryptophanes in dioxane (a solvent too bulky to enter the cavity) and evaporating off the solvent under vacuum (100 °C). Then the CD spectra of the empty hosts were recorded in dioxane and those of the $CHCl_3$ complexes in a dioxane/$CHCl_3$ mixture (8:2, v/v).[23] No significant differences were found for **2** and **3**, and only weak changes in the intensities of several bands were noticed between the spectra of empty **1** and its $CHCl_3$ complex; we shall return to these results below.

As can clearly be seen in Figures 1–6, the $B_{2u}$ and $B_{1u}$ aromatic transitions in the CD spectra of **1**–**6** can easily be identified by comparison with the UV data (Table II). On the higher energy side, the CD bands of the $B_{1u}$ system are well separated from the allowed benzene transitions[25] (below 230 nm), whereas in the UV spectra the $B_{1u}$ system is extensively overlapped by these transitions.

In the $B_{1u}$ region, the (−)-cryptophanes **1**–**6** show two oppositely signed CD bands between ca. 230 and 260 nm; from high to low energy, the sequence of signs is positive–negative for all compounds but the hexaphenol **4** (and the corresponding sodium hexaphenoxide), for which the sequence is reversed.

In the $B_{2u}$ region, the picture seems, at first glance, more complex. The compounds **2** and **5** display two broad, oppositely signed bands, with a positive–negative sequence from high to low energy (ca. 275–300 nm). In the case of **1**, two negative Cotton effects (CE's) are observed, with the minimum in between (reaching zero in the spectrum of the $CHCl_3$ complex) corresponding to the maximum of the UV absorption (288 nm). In **6**, a single negative CE is visible at 297 nm, and the CD is *flat* between 265 and 280 nm, the UV maximum being at 286 nm. All these features could be explained by the presence of two negative bands and one positive band; in **1**, the latter is partially cancelled by the two dominant negative CE's, whereas in **6** the positive and negative CE's at higher energy totally cancel each other, leaving a single negative band at low energy. This idea of three bands in this region is supported by the spectra of the hexaphenol **4** and of its hexaphenoxide (Figure 4), in which a central positive band is now well visible in addition to two negative components. Likewise, the $B_{2u}$ CD of **3** shows two negative bands and one positive band, but the latter is now found at lower energy and is very close to the central negative CE evidenced by a shoulder at 292 nm; these two bands seem to have suffered extensive overlap and mutual cancellation.

Summarizing, the CD spectra of the cryptophanes in the $B_{2u}$ region seem to consist of a nonconservative *bisignate* system of *three* bands; in the case of (−)-**1**, **3**, **4**, and **6**, the presence of two negative CE's and one positive CE has been evidenced, while for **2** and **5** there has been no clear experimental indication in favor of the same or of the inverse (two positive CE's, one negative CE) situation. Moreover, the relative locations (i.e. the relative energies) of these components may vary from one cryptophane to another, and the extent to which the three bands overlap and

(23) The binding constants of the 1:1 $CHCl_3$ complexes of **1** and **2** in 1,1,2,2-tetrachloroethane are ca. 230 and 470 L/mol, respectively, at 300 K;[18,24] that of the corresponding complex of **3** is not known.

(24) Canceill, J.; Lacombe, L.; Collet, A. *J. Chem. Soc., Chem. Commun.* **1987**, 219–221.

(25) The CD associated with the allowed benzene transitions will not be discussed in this paper, because the effect of the substituents on the polarization of these transitions is not experimentally known.

**Chart II.** Reference System, as Viewed Down the $z$ Axis

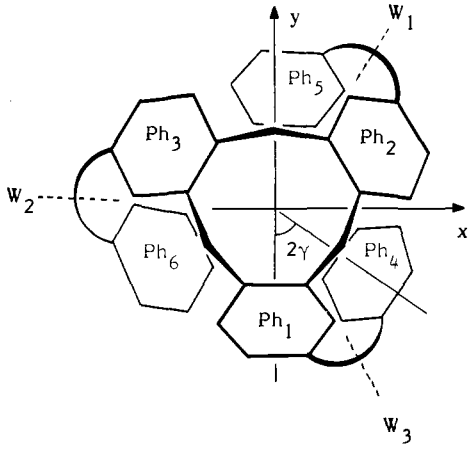


mutually cancel each other presumably accounts for the various spectral figures observed in the $B_{2u}$ region.

### Coupled-Oscillator Approach to the Optical Activity of $D_3$-Cryptophanes

We first describe the geometry of the cryptophanes and define the reference system used in the theoretical treatment given below. In Chart II, the idealized $D_3$ structure of the molecular frame is viewed along the $C_3$ axis ($z$ axis). The $yz$ plane bisects the benzenic unit $Ph_1$ of the upper cap, and the $x$ and $y$ axes define the equatorial plane containing the three $C_2$ axes $W_1$–$W_3$. The upper and lower caps are twisted away from the eclipsed conformation by angle $2\gamma$. This ideal $D_3$ geometry has been almost exactly observed by X-rays for cryptophane E (**2**) ($CHCl_3$ complex);[19] the propylenedioxy bridges displayed a $C_2$ conformation, and $2\gamma$ was 58° (i.e. staggered conformation). For **1** and its derivatives **4–6** no X-ray data are presently available, and we could not firmly establish through variable-temperature $^1H$ NMR experiments whether the preferred conformation of the ethylenedioxy chains was anti or gauche. Although the latter is normally more stable, we suspect that steric hindrance due to the adjacent methoxy groups might favor the anti conformation in this case. In the analogous compound cryptophane C (**13**), where one of the caps is devoid of methoxy groups, an X-ray study of the dichloromethane inclusion complex[16] revealed that two of the bridges were gauche and the third anti, which in fact resulted in a better host–guest fit. The anti conformation is ca. 0.8 Å longer (which slightly enlarges the cavity and favors guest inclusion), but CPK models clearly show that this difference has little consequence on the twist angle $2\gamma$, which in cryptophane C was 52°. The small difference in the CD intensities on going from *empty* **1** to its chloroform complex (Figure 1) perhaps corresponds to a similar conformational change of the chains (from gauche to anti) on complexation. We assume, however, that in both situations the twist angle remains the same and is similar to that found in cryptophane C (the same holds true for **4–6**). In cryptophane G (**3**), where the chains are slightly longer, the most probable consequence, as CPK models suggest, is that the two caps are wrapped around the $C_3$ axis so as to keep the distance between them nearly constant. This would only result in a small increase of $2\gamma$ to a value close to 60°.

In order to complete the description of the system, we need to know the distances between the centers of the phenyl rings of the same ($d_{12}$) and of different ($d_{14}$) caps and the value of angle $\phi$, at the top of the cyclotribenzylene crowns (Chart III). In all compounds, $\phi \sim 48°$ and $d_{12} \sim 4.79$ Å, while $d_{14}$ is in the range 6.5–7.5 Å on going from **1** and **4–6** to **2** and **3**.

**Ground- and Excited-State Wave Functions.** We regard the cryptophanes as formed of two groups of fragments: the nonaromatic frame (i.e. the chains) and the substituted benzene rings of the upper and lower caps. Accordingly, the ground-state molecular wave function is given by (1), where $\Phi_0$ represents the

$$\Psi_0 = A\{\Phi_0, \Phi_1, ..., \Phi_6\} \quad (1)$$

**Chart III.** Reference System and Radial Vector $\mathbf{R}^1$ for the Benzene Ring $Ph_1$, Whose Plane Is Parallel to the $x$ Axis

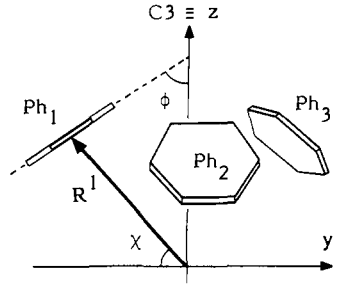


**Chart IV.** Polarization Angles $\theta$ and $\theta'$ for the $B_{2u}$ and $B_{1u}$ Transitions, Respectively[a]

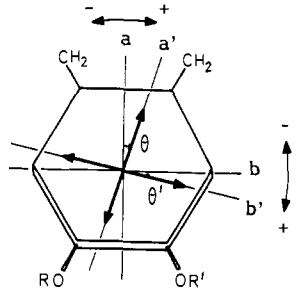


[a] For the absolute configuration of the (−)-cryptophanes **1–6**, substituent R is either H, Me, or Ac and R′ is the chain bridging the two cyclotribenzylene caps.

nonaromatic frame and $\Phi_1$–$\Phi_6$ the benzene rings, the overall antisymmetry requirement of the wave function being satisfied through the operator $A$. Each fragment is characterized by well-defined spectral properties. The excitation frequencies of the nonaromatic frame (>50 000 $cm^{-1}$) are much higher than those of the benzene rings (30 000–40 000 $cm^{-1}$); for instance, the excited wave function (2) represents an excitation localized on the $i$th

$$\Psi_b{}^i = A\{\Phi_0, \Phi_1, ..., \Phi_i{}^*, ..., \Phi_6\} \quad (2)$$

benzene ring. We shall limit our discussion to the two lowest transitions of the chromophore, which occur at frequencies $\bar{\nu}_a$ and $\bar{\nu}_b$, respectively, with their transition moments roughly along the short ($a$) and long ($b$) axes shown in Chart IV. These transitions will hereafter be designated $B_{2u}$ ($a$) and $B_{1u}$ ($b$) as in the parent benzene molecule. We disregard charge-transfer effects and locate the transition dipoles at the centers of the benzene rings, whose positions are defined by the radial vectors $\mathbf{R}^i$ (Chart III). For the benzene ring $Ph_1$, the components of $\mathbf{R}^1$ in the reference system $(0, -\mathbf{R}^1 \cos \chi, \mathbf{R}^1 \sin \chi)$ are easily related to the structural parameters by the expressions

$$3^{1/2}\mathbf{R}^1 \cos \chi = d_{12}$$

$$2(3^{1/2})\mathbf{R}^1 \sin \chi = [3d_{14} - 2d_{12}(1 - \cos 2\gamma)]^{1/2}$$

Due to the presence of the substituents (Chart IV), the dipoles of the $B_{2u}$ and $B_{1u}$ transitions lie along the $a'$ and $b'$ directions, making the angles $\theta$ and $\theta'$ with the $a$ and $b$ axes, respectively. The directions of the transition dipoles in benzene ring $Ph_1$ are therefore

$$B_{2u}: \sin \theta, \cos \theta \sin \phi, \cos \theta \cos \phi$$

$$B_{1u}: \cos \theta', -\sin \theta' \sin \phi, -\sin \theta' \cos \phi$$

**Symmetry and Expression of the Excited-State Wave Functions.** We now consider two cases for the description of the excited states: (i) a first-order model, which corresponds to a selective excitation of only a single transition for frequencies close to either $\bar{\nu}_a$ or $\bar{\nu}_b$; and (ii) a second-order model, where both transitions are simultaneously excited for any frequency in the range $\bar{\nu}_a$, $\bar{\nu}_b$.

The irreducible representation of the $D_3$ group provides a convenient way to classify the ground and excited states, and properly symmetrized wave functions for each symmetry state $\Gamma$

**Table III.** $A_1$, $A_2$, and E Standard Irreducible Representations of the $D_3$ Group; Angle $\gamma$ and $W(c_2)$ Symmetry Axes Defined in Chart II[a]

| | $E$ | $C_3$ | $C_3^2$ | $W_1$ | $W_2$ | $W_3$ |
|---|---|---|---|---|---|---|
| $A_1$ | 1 | 1 | 1 | 1 | 1 | 1 |
| $A_2$ | 1 | 1 | 1 | −1 | −1 | −1 |
| E | $\begin{pmatrix}1 & 0\\ 0 & 1\end{pmatrix}$ | $\begin{pmatrix}-1/2 & 3^{1/2}/2\\ -3^{1/2}/2 & -1/2\end{pmatrix}$ | $\begin{pmatrix}-1/2 & -3^{1/2}/2\\ 3^{1/2}/2 & -1/2\end{pmatrix}$ | $\begin{pmatrix}a & b\\ b & -a\end{pmatrix}$ | $\begin{pmatrix}-\cos 2\gamma & \sin 2\gamma\\ \sin 2\gamma & \cos 2\gamma\end{pmatrix}$ | $\begin{pmatrix}c & d\\ d & -c\end{pmatrix}$ |

[a] Key: $a = 1/2 \cos 2\gamma + 3^{1/2}/2 \sin 2\gamma$; $b = -1/2 \sin 2\gamma + 3^{1/2}/2 \cos 2\gamma$; $c = 1/2 \cos 2\gamma - 3^{1/2}/2 \sin 2\gamma$; $d = -1/2 \sin 2\gamma - 3^{1/2}/2 \cos 2\gamma$.

**Table IV.** Excited-State Wave Functions of Various Symmetry Species

| | | |
|---|---|---|
| $A_1$ | | $(1/6^{1/2})[\Psi_b^1 + \Psi_b^2 + \Psi_b^3 + \Psi_b^4 + \Psi_b^5 + \Psi_b^6]$ |
| $A_2$ | | $(1/6^{1/2})[\Psi_b^1 + \Psi_b^2 + \Psi_b^3 - \Psi_b^4 - \Psi_b^5 - \Psi_b^6]$ |
| E | $x$ | $(1/12^{1/2})[2\Psi_b^1 - \Psi_b^2 - \Psi_b^3 - (2\cos 2\gamma)\Psi_b^4 + (\cos 2\gamma - 3^{1/2}\sin 2\gamma)\Psi_b^5 + (\cos 2\gamma + 3^{1/2}\sin 2\gamma)\Psi_b^6]$ |
| | $y$ | $(1/2)[\Psi_b^2 - \Psi_b^3 + ((2/3^{1/2})\sin 2\gamma)\Psi_b^4 - (\cos 2\gamma + (1/3^{1/2})\sin 2\gamma)\Psi_b^5 + (\cos 2\gamma - (1/3^{1/2})\sin 2\gamma)\Psi_b^6]$ |
| E | $x$ | $(1/2)[-\Psi_b^2 + \Psi_b^3 + (2/3^{1/2})\sin 2\gamma)\Psi_b^4 - (\cos 2\gamma + (1/3^{1/2})\sin 2\gamma)\Psi_b^5 + (\cos 2\gamma - (1/3^{1/2})\sin 2\gamma)\Psi_b^6]$ |
| | $y$ | $(1/12^{1/12})[2\Psi_b^1 - \Psi_b^2 - \Psi_b^3 + (2\cos 2\gamma)\Psi_b^4 - (\cos 2\gamma - 3^{1/2}\sin 2\gamma)\Psi_b^5 - (\cos 2\gamma + 3^{1/2}\sin 2\gamma)\Psi_b^6]$ |

**Table V.** Electric ($\mu_{ab}$) and Magnetic ($m_{ab}$) Transition Moments and Rotation Strengths in Reduced Units for $B_{2u}$ and $B_{1u}$ Transitions ($x$, $y$, $z$ Indicate Polarization Directions and $\mu_{b'}$ Indicates the $B_{1u}$ Transition Moment (Modulus) in Reduced Units)

| | | $\mu^\Gamma$ | $m^\Gamma$ | $R^\Gamma$ |
|---|---|---|---|---|
| $B_{2u}$ | $A_1$ | 0 | 0 | 0 |
| | $A_2(z)$ | $6^{1/2}\cos\theta\cos\phi$ | $6^{1/2}\lvert\mathbf{R}\rvert\sin\theta\cos\chi$ | $3\lvert\mathbf{R}\rvert\sin 2\theta\cos\chi\cos\phi$ |
| | $E(x)$ | $3^{1/2}\sin\theta$ | $-3^{1/2}\lvert\mathbf{R}\rvert\cos\theta\cos(\phi-\chi)$ | $-(3/2)\lvert\mathbf{R}\rvert\sin 2\theta\cos(\phi-\chi)$ |
| | $E(y)$ | $3^{1/2}\sin\theta$ | $-3^{1/2}\lvert\mathbf{R}\rvert\cos\theta\cos(\phi-\chi)$ | $-(3/2)\lvert\mathbf{R}\rvert\sin 2\theta\cos(\phi-\chi)$ |
| | $E(x)$ | $3^{1/2}\cos\theta\sin\phi$ | $3^{1/2}\lvert\mathbf{R}\rvert\sin\theta\sin\chi$ | $(3/2)\lvert\mathbf{R}\rvert\sin 2\theta\sin\chi\sin\phi$ |
| | $E(y)$ | $3^{1/2}\cos\theta\sin\phi$ | $3^{1/2}\lvert\mathbf{R}\rvert\sin\theta\sin\chi$ | $(3/2)\lvert\mathbf{R}\rvert\sin 2\theta\sin\chi\sin\phi$ |
| $B_{1u}$ | $A_1$ | 0 | 0 | 0 |
| | $A_2(z)$ | $-6^{1/2}\mu_{b'}\sin\theta'\cos\phi$ | $6^{1/2}\lvert\mathbf{R}\rvert\mu_{b'}\cos\theta'\cos\chi$ | $-3\lvert\mathbf{R}\rvert\mu_{b'}^2\sin 2\theta'\cos\chi\cos\phi$ |
| | $E(x)$ | $3^{1/2}\mu_{b'}\cos\theta'$ | $3^{1/2}\lvert\mathbf{R}\rvert\mu_{b'}\sin\theta'\cos(\phi-\chi)$ | $(3/2)\lvert\mathbf{R}\rvert\mu_{b'}^2\sin 2\theta'\cos(\phi-\chi)$ |
| | $E(y)$ | $3^{1/2}\mu_{b'}\cos\theta'$ | $3^{1/2}\lvert\mathbf{R}\rvert\mu_{b'}\sin\theta'\cos(\phi-\chi)$ | $(3/2)\lvert\mathbf{R}\rvert\mu_{b'}^2\sin 2\theta'\cos(\phi-\chi)$ |
| | $E(x)$ | $-3^{1/2}\mu_{b'}\sin\theta'\sin\phi$ | $3^{1/2}\lvert\mathbf{R}\rvert\mu_{b'}\cos\theta'\sin\chi$ | $-(3/2)\lvert\mathbf{R}\rvert\mu_{b'}^2\sin 2\theta'\sin\chi\sin\phi$ |
| | $E(y)$ | $-3^{1/2}\mu_{b'}\sin\theta'\sin\phi$ | $3^{1/2}\lvert\mathbf{R}\rvert\mu_{b'}\cos\theta'\sin\chi$ | $-(3/2)\lvert\mathbf{R}\rvert\mu_{b'}^2\sin 2\theta'\sin\chi\sin\phi$ |

($\Gamma = A_1, A_2, E$) are obtained from (2) through the symmetry projection (3), where $n$ is the dimension of the $\Gamma$-irreducible

$$\Psi_{a(b)}{}^\Gamma = (n^\Gamma/g)\sum_{\hat{R}} D_{1k}{}^*(\hat{R})\hat{R}\,\Psi'_{a(b)} \tag{3}$$

representation, $g$ is the number of symmetry operations of the molecular point group, and $D_{1k}(\hat{R})$ are the matrix elements of the corresponding symmetry operator $\hat{R}$ (Table III). This expression simply means that the $\hat{R}$ operator transforms a localized excitation $\Psi_{a(b)}$ into an equivalent excitation in another benzene unit, producing the set of excited wave functions shown in Table IV.

In the first-order description, the expression of the molecular wave functions of the excited states is completely determined by the symmetry elements of the $D_3$ group. Since the ground state is totally symmetric, the electric and the magnetic transition moments to reach the excited states (Table IV) can be simply obtained by applying the symmetry operator $\hat{R}$ to the electric $\mu_{a'(b')}{}^1$ and magnetic $m_{a'(b')}{}^1$ moments localized in the benzene unit $Ph_1$ (eq 4 and 5). The magnetic moment $m_{a'(b')}{}^1$ in (5) can be

$$\mu_{a'(b')}{}^\Gamma = (n^\Gamma/g)\sum_{\hat{R}} D_{1k}{}^*(\hat{R})\hat{R}\mu_{a'(b')}{}^1 \tag{4}$$

$$m_{a'(b')}{}^\Gamma = (n^\Gamma/g)\sum_{\hat{R}} D_{1k}{}^*(\hat{R})\hat{R}m_{a'(b')}{}^1 \tag{5}$$

evaluated by using eq 6, which is equivalent to a point–dipole

$$m_{a'(b')}{}^1 = i\pi\bar{\nu}_{a(b)}\mathbf{R}^1 \times \mu_{a'(b')}{}^1 \tag{6}$$

approximation and to a length representation of the momentum operator.[26] From expressions 4 and 5, the rotational $R$ and dipole $D$ strengths of the $B_{2u}(a')$ and $B_{1u}(b')$ transitions can now be calculated (eq 7 and 8). The analytical expressions for the electric and magnetic transition dipoles and the rotational strengths are given in Table V, as a function of $\theta$ and $\theta'$ and of the structural parameters of the system

$$R_{a'(b')}{}^\Gamma = \mathrm{Im}(m_{a'(b')}\cdot\mu_{a'(b')}) \tag{7}$$

$$D_{a'(b')}{}^\Gamma = \mu_{a'(b')}\cdot\mu_{a'(b')} \tag{8}$$

**Excited-State Energies.** Not only the signs and intensities of the rotational strengths but also the energy sequence of the excited states are essential for determining the shape of the CD spectra. When small terms due to antisymmetry are neglected, the energy sequence of the excited states can be calculated by the two-electron matrix elements $\langle\Phi_i\Phi_j{}^*|1/r_{12}|\Phi_i{}^*\Phi_j\rangle$, which in the dipole approximation are written

$$|\mathbf{R}^j - \mathbf{R}^i|^{-3}\mu_{a'}{}^i\cdot\mu_{a'}{}^j - 3|\mathrm{R}^j - \mathrm{R}^i|^{-5}\,(\mu_{a'}{}^i\cdot(\mathrm{R}^j - \mathrm{R}^i))(\mu_{a'}{}^j\cdot(\mathbf{R}^j - \mathbf{R}^i))$$

with a similar expression for the $\mu_{b'}{}^i$, $\mu_{b'}{}^j$ interactions.

In the first-order description, only three types of pairwise interactions corresponding to ($Ph_1$–$Ph_2$), ($Ph_1$–$Ph_4$), and ($Ph_1$–$Ph_6$) are required to describe all the energy states of the $B_{2u}$ and $B_{1u}$ manifolds in the $D_3$ point group. In the second-order description, three additional pairwise interactions between the $\mu_{a'}{}^i$ and $\mu_{b'}{}^j$ transition dipoles are necessary to set up the 2 × 2 secular equations for each symmetry state, from which the energies and wave functions can be derived.

**Theoretical CD Spectra.** We emphasize that in this treatment the chirality of the $B_{2u}$ and $B_{1u}$ oscillator arrays originates exclusively from the rotations $\theta$ and $\theta'$ of the transition dipoles in each aromatic ring. If $\theta$ and $\theta'$ are set to zero, then no optical activity will be generated by the coupled-oscillator model, even though the molecular frame is still structurally chiral (because

(26) Eyring, W.; Walter, J.; Kimball, G. E. *Quantum Chemistry*; Wiley: New York, 1960; p 111.
(27) Collet, A.; Gottarelli, G. *J. Am. Chem. Soc.* **1982**, *104*, 7383–7384.
(28) Platt, J. R. *J. Chem. Phys.* **1951**, *19*, 263–271.
(29) Sagiv, J. *Tetrahedron* **1977**, *33*, 2303–2313; *Ibid.* **1977**, *33*, 2315–2320.
(30) The spectroscopic moment of an acetoxy group is ca. +10 (L/mol·cm)$^{1/2}$ and that of a methoxy group ca. +30 (L/mol·cm)$^{1/2}$. See ref 29.
(31) Brickell, W. S.; Mason, S. F.; Roberts, D. R. *J. Chem. Soc. B* **1971**, 691–695.
(32) All necessary details for these calculations have been given in ref 10. In this paper, however, the final equation used for plotting the CD curves contains a printing error. The correct expression is $\Delta\epsilon(\tilde{\nu}) = ((18.8 \times 10^{37})/P)\sum_i(R_i(\bar{\nu}_i)^{1/2})\exp[-(\tilde{\nu} - \bar{\nu}_i)^2/2P^2\bar{\nu}_i]$.

**Table VI.** Computed Energies ($E$), Dipole ($D$), and Rotational ($R$) Strengths in Reduced Units: (a, b, c) First-Order and (d) Second-Order Calculations[a]

| | | (a) ($d_{14}$ = 1.4, 2$\gamma$ = 0°) | | | (b) ($d_{14}$ = 1.4, 2$\gamma$ = 60°) | | | (c) ($d_{1.4}$ = 1.6, 2$\gamma$ = 60°) | | | (d) ($d_{14}$ = 1.60, 2$\gamma$ = 60°) | | |
|---|---|---|---|---|---|---|---|---|---|---|---|---|---|
| | | $E$ | $D$ | $R$ | $E$ | $D$ | $R$ | $E$ | $D$ | $R$ | $E$ | $D$ | $R$ |
| $B_{2u}$ | E | −2.056 | 0.016 | −0.284 | −1.767 | 0.016 | −0.270 | −1.686 | 0.016 | −0.396 | −1.686 | 0.015 | −0.286 |
| | E | −0.757 | 3.304 | 0.163 | −1.047 | 3.304 | 0.149 | −1.128 | 3.304 | 0.174 | −1.128 | 3.304 | 0.168 |
| | $A_2$ | 2.537 | 2.679 | 0.121 | 2.680 | 2.679 | 0.121 | 2.693 | 2.679 | 0.121 | 2.692 | 2.680 | 0.139 |
| | $A_1$ | 3.090 | 0 | 0 | 2.948 | 0 | 0 | 2.935 | 0 | 0 | 2.935 | 0 | 0 |
| $B_{1u}$ | $A_1$ | 12.878 | 0 | 0 | 13.236 | 0 | 0 | 13.110 | 0 | 0 | 13.110 | 0 | 0 |
| | $A_2$ | 13.151 | 0.007 | 0.162 | 12.793 | 0.007 | 0.162 | 12.919 | 0.007 | 0.162 | 12.919 | 0.005 | 0.144 |
| | E | 19.471 | 0.008 | 0.218 | 20.016 | 0.008 | 0.198 | 20.095 | 0.008 | 0.231 | 20.095 | 0.008 | 0.238 |
| | E | 21.514 | 11.982 | −0.379 | 20.969 | 11.982 | −0.360 | 20.890 | 11.982 | −0.394 | 20.890 | 11.982 | −0.402 |

[a] Parameters used for calculation: $d_{12}$ = 4.79 Å, $\theta$ = 3°, $\theta'$ = −2°, $\phi$ = 48°, $\mu_{b'}$ = 2, $E(B_{1u}) - E(B_{2u})$ = 18 reduced energy units.

of the topology of the chains linking the caps).[33] In the same way, changing the signs of $\theta$ and $\theta'$ produces *enantiomeric* spectra in this model (see the dependence of the rotational strengths in Table V), while strictly speaking *diastereoisomeric* (or quasi-enantiomeric) spectra would be expected if all the structural features of the molecule (especially the chains) were taken into account. Nevertheless, the model is justified because the coupled-oscillator mechanism is dominant in the considered spectral region.

Changes in the structural parameters 2$\gamma$ and $d_{14}$ may affect the spectra by altering the band intensities and the sequence of the excited states without affecting the *signs* of the CD bands. In order to illustrate this point, we found it convenient to use reduced units for calculating the UV and CD spectra predicted by the model. Reduced units for the energies ($d_{12}^{-3}|\mu|^2$), for the dipole strengths ($|\mu|^2$), and for rotational strengths ($\pi\bar{\nu}d_{12}|\mu|^2$) were obtained by scaling the inter-ring distances by $d_{12}$ and the transition dipole strengths by $|\mu_{a'}|$. Realistic values for $|\mu_{a'}|$, $|\mu_{b'}|$, $\bar{\nu}_{a'}$, and $\bar{\nu}_{b'}$ were obtained from the UV absorption intensities and frequencies of suitable monomer models as previously described.[10-12] Typical results are assembled in Table VI. In all these calculations, $\theta$ and $\theta'$ were arbitrarily given the values +3° and −2°, respectively (see Chart IV for the sign definition), and the energy difference between the barycenters of the $B_{2u}$ and $B_{1u}$ systems was set to 18 reduced energy units.

We conclude the following: (i) In the zero-order description, each of the $B_{2u}$ and $B_{1u}$ systems is always split into a bisignate set of three components ($A_2$, E, E). The $A_2$ component is at higher energy in the $B_{2u}$ system and at lower energy in the $B_{1u}$ system. (ii) The sequence of signs of the three components in each band system is (++−) for the $B_{2u}$ and (+−−) for the $B_{1u}$ transition, from high to low energy, when the corresponding angle $\theta$ or $\theta'$ is positive. (iii) The influence of the twist angle 2$\gamma$ on the band intensities is negligible. (iv) In both band systems, the separation of the pair of E components is small compared to the energy difference between the E and $A_2$ levels. (v) The separation of the E levels significantly depends on the twist angle 2$\gamma$. It is much larger for 2$\gamma$ = 0° than for 60°, where the two components become nearly degenerate. Moreover, the separation is further reduced by increasing the inter-ring distance $d_{14}$. (vi) In the second-order treatment, the calculated CD for each transition is no longer conservative. There is a transfer of intensity from the $A_2$ component of the $B_{1u}$ transition to the $A_2$ component of the $B_{2u}$ system, while for the E component some intensity is transferred from the $B_{2u}$ to the $B_{1u}$ transition. However, the exchange of intensity is small.

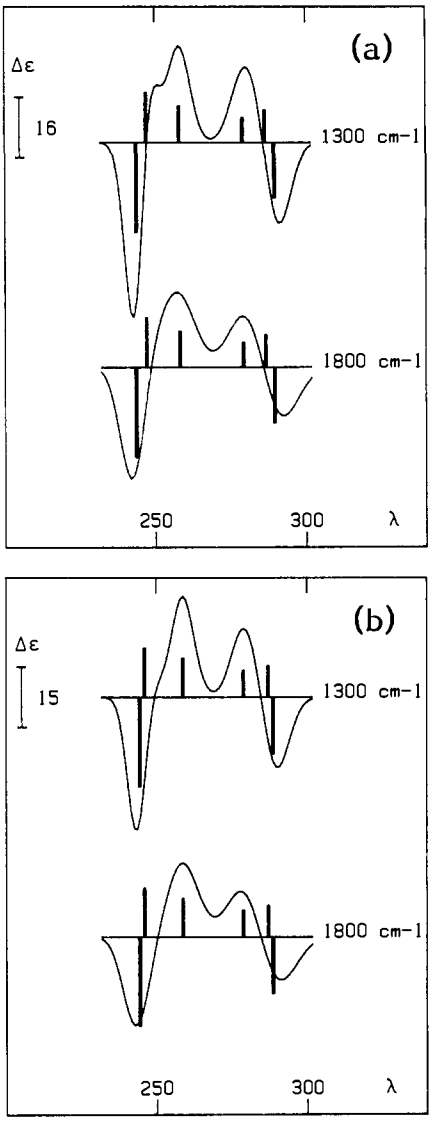


**Figure 7.** Bandwidth dependence of the theoretical CD curves for eclipsed (a) and staggered (b) conformations of $D_3$-cryptophanes.

In order to see the effect of twist angle variations on the spectra, theoretical CD curves for 2$\gamma$ = 0 and 60°((a) and (b) respectively, in Table VI) were plotted by using the band shape function proposed by Mason,[6,31,32] assuming that the spectrum is the sum of Gaussian bands. Typical curves are shown in Figure 7. For 2$\gamma$ = 60° (staggered conformation), the spectrum consists for each benzene transition of a bisignate couplet, where the $A_2$ component and the largest E component determine the sequence of signs. No resolution of the E components in each band system could be

(33) Three elements of chirality can be identified in $D_3$-cryptophanes: (1) Ignoring the chains and the substituents, the twist angle 2$\gamma$ determines a *conformational helicity* (*M* or *P*), which disappears when 2$\gamma$ = 0° or 60° (like in biphenyl for 0° or 90°). (2) Branching the chains introduces a *structural element* of chirality, which is independent of 2$\gamma$ (like in a bridged biphenyl), and the handedness of the molecule is determined by the bridge connections (e.g., compare formula I and its mirror image). (3) Finally, the polarization direction $\theta$ of the transition dipoles is also a structural element of chirality, which determines the handedness of the oscillator array. This handedness is not modified by changes of 2$\gamma$, which only cause a modulation of the chiroptical intensities. The mathematical reason of the zero circular dichroism when $\theta$ = 0 is found in Table V. *Either* the magnetic *or* the electric moment vanishes, whatever the coupling ($A_2$, E, E) of the oscillator array. The physical meaning of this result can only be seen easily in the case of the symmetrical $A_2$ coupling, by using the pictorial representation of Figure 8 and setting $\theta$ to zero; the magnetic moment along the $C_3$ axis then vanishes. A similar representation for the E coupling modes is not so easy to understand, hence the usefulness of the mathematical treatment.

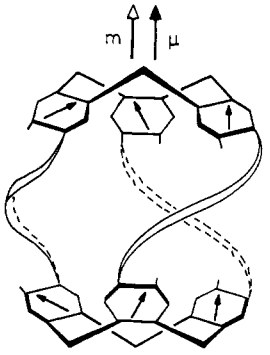


**Figure 8.** Pictorial representation of the origin of the positive $A_2$ component of the $B_{2u}$ transition when $\theta > 0$. The coupling of the individual dipoles generates along the $z$ direction parallel magnetic ($m$) and electric ($\mu$) moments.

obtained in such simulations for any realistic choices of bandwidths (1300–1800 $cm^{-1}$). For $2\gamma = 0°$ (eclipsed conformation), where the E states split apart, this splitting becomes apparent in the $B_{1u}$ system when small bandwidths are used (1300 $cm^{-1}$); even in this case, the E states of the $B_{2u}$ system are not resolved.

As in the $C_3$-cyclotriveratrylenes, the interaction energy of the transition dipoles depends on the magnitude of $\theta$ and $\theta'$, and there is a "magic angle" $\theta_m$ (or $\theta'_m$), at which all levels become degenerate and beyond which the position of the components is totally inverted.[10,27] The value of the magic angle in the cryptophanes is similar to that of the cyclotriveratrylene units (ca. 45°) and is actually too large to be reached in these compounds, for any kind of substituents.

Finally, a pictorial representation of the origin of the positive rotational strength of the $A_2$ component of the $B_{2u}$ transition for $\theta$ positive is depicted in Figure 8.

## Discussion

Following Platt's spectroscopic moment theory,[28] the intensity of the forbidden $B_{2u}$ and $B_{1u}$ benzene transitions mainly originates from substituent effects. In the cryptophanes (as in the parent cyclotriveratrylenes) each absorbing unit is a 1,2,4,5-tetrasubstituted benzene. The two $CH_2$ groups (see Chart IV) can be considered equal, and the magnitudes of $\theta$ and $\theta'$ therefore should depend only on the relative magnitude of the spectroscopic moments (sm) of the OR and OR′ substituents. The validity of this simple theory in this class of compounds has been well established for the $B_{2u}$ transition;[10-12] namely, the rotation of the transition dipole (Chart IV) will be clockwise if the spectroscopic moment of OR′ is greater than that of OR. The situation of the $B_{1u}$ transition is more complex. It is often assumed that the $B_{1u}$ and $B_{2u}$ dipoles are orthogonally polarized (i.e., $\theta = \theta'$), which is simply equivalent to saying that the substituent sm have the same magnitude for both transitions. In fact, as was pointed out by Sagiv[29] and experimentally demonstrated in our previous works,[10-12] the influence of the substituents is not the same for the two transitions and there is no reason why $\theta$ should be equal to $\theta'$ when OR is different from OR′ (see Chart IV). This problem is particularly relevant here, because, in several of the cryptophanes studied (e.g. **1–4**), $\theta$ and $\theta'$ are close to zero, a value at which the chirality of the oscillator array is inverted. On the other hand, since the absolute configurations of these compounds are known, we may expect that, by using the present model to analyze the CD spectra, reliable information is obtained about the polarization of the transitions.

In the following discussion, we shall consider three typical situations: (i) The signs of $\theta$ and $\theta'$ can be *unambiguously* established a priori from the known sm of the substituents. (ii) The signs of $\theta$ and $\theta'$ obtained from the works on chiral cyclotriveratrylenes[10] are consistent with the present CD spectra. (iii) All remaining cases for which tentative assignments will be proposed.

**(i) Hexaacetate (−)-5.** The sm of the acetoxy group being much smaller than that of the alkoxy chains,[30] there is no ambiguity as to the signs of $\theta$ and $\theta'$, which for the absolute configuration depicted, should both be *positive*. In the analogous cyclotriguaiacylene triacetate (**12**),[10] the magnitude of $\theta$ and $\theta'$ has been estimated to be ca. 25°; although in **5** this figure should be somewhat reduced (to perhaps 15–20° or less) because the sm of the alkoxy chain in the cryptophane is probably smaller than that of the methoxy group in **12**, this difference has no bearing on the CD signs since only the intensities are affected by such variations of $\theta$ and $\theta'$. For (−)-**5**, the comparison of the calculated (with $\theta = \theta' = 15°$) and experimental spectra seems straightforward (Figure 5). The negative band at 244.5 nm should correspond to the calculated $A_2$ component of the $B_{1u}$ transition, while the positive band at 230.5 nm is likely to be the resultant of the two almost degenerate E components where the positive part prevails.

For the $B_{2u}$ system, the positive band at 271.5 nm in our scheme represents the $A_2$ component, and the negative band at lower energy would then result from the partial cancellation of the two E components. These assignments are substantiated by the very good agreement between the signs, shapes, and even intensities of the experimental and theoretical CD curves. In particular, no resolution of the E components in the $B_{1u}$ band system could be evidenced in the computed spectra, for realistic bandwidths; this results in an indirect confirmation of a staggered conformation of the cryptophane in solution.

**(ii) Cryptophanes 1, 3, and 4.** The sm of the methoxy group and of the alkoxy chain being of the same order of magnitude, $\theta$ and $\theta'$ in these compounds are probably very small. In $C_3$-cyclotriveratrylenes bearing two OR and OR′ substituents (R and R′ ≠ H), we have established that, for the $B_{2u}$ transition, the sm of the smallest alkoxy group was greater than that of the bulkier group (e.g., $OCH_3$ vs $OC_2H_5$), the situation being *reversed*, however, for the $B_{1u}$ transition. If the same behavior holds for (−)-**1** and (−)-**3**, then $\theta$ should be *negative* and $\theta'$ *positive*, as sketched in the inserts of Figures 1 and 3.

With use of these signs, the agreement between the theoretical model and the experimental CD is nearly perfect in the case of (−)-**3** (Figure 3). For the $B_{2u}$ system, the observed (−−+) sequence matches the calculated $A_2$, E, E components exactly; for the $B_{1u}$ system, the negative band at 253.5 nm corresponds to the calculated $A_2$ component, while the positive band at 237 nm should represent the sum of the E components, with the positive one being dominant.

As shown in Figure 1 for (−)-**1**, the agreement is good for the $B_{1u}$ system. For the $B_{2u}$ transition only the $A_2$ component corresponding to a negative band is predicted at the experimental frequency; instead, the two E components at lower energy are probably inverted. In fact, the splitting between the two E components is calculated to be very small (ca. 1 nm), and the validity of the point-dipole approximation in such a situation is questionable.

We now turn to the hexaphenol (−)-**4** (Figure 4). According to the earlier data on the CD of the parent triphenol **9**, $\theta$ and $\theta'$ in (−)-**4** should both be *negative*. Also, this assignment seems consistent with the model, which in this case predicts for the $B_{1u}$ system a negative component at higher energy (the sum of two nearly degenerate E transitions with a strong negative component), followed by a positive $A_2$ transition. This sequence of signs is indeed observed in the experimental spectrum. The fact that the experimental $B_{1u}$ CD is very weak probably means that $\theta'$ in **4** is very small, perhaps less than −0.5°, as suggested by the spectra simulations. For the $B_{2u}$ system, the predicted negative $A_2$ component is observed (277.5 nm), and as in **1**, the two E components are probably inverted with respect to the computed sequence.

After ionization of the phenolic groups (in the presence of sodium methoxide in methanol), the CD spectrum of (−)-**4** is red-shifted and shows enhanced intensities, but the sequence of signs remains the same as before ionization. This behavior, which is similar to that of the parent triphenol **9**, should probably be interpreted in the same way,[10,27] in terms of a larger sm for the ionized than for the un-ionized OH groups, which in turn makes $\theta$ and $\theta'$ more negative, as illustrated in Figure 4.

**(iii) Cryptophanes 2 and 6.** For the same reason as in (ii), angles $\theta$ and $\theta'$ are probably very small. In the $B_{1u}$ region, the CD spectra of (−)-**2** and (−)-**6** (Figures 2 and 6) display the same sequence of signs as observed in **1**, **3**, and **4**, and $\theta'$ in these compounds is probably *positive*, as expected. For the $B_{2u}$ system, the experimental spectrum of (−)-**2** is correctly simulated only when $\theta$ is given a *positive* sign, corresponding to a greater sm of the $O(CH_2)_3$ chain compared to the $OCH_3$ group. Although in contrast with previous results, this observation is justified since the X-ray structure[19] of this cryptophane shows the near coplanarity of the $OCH_2$ bond with the phenyl ring. The sequence of sm of the two substituents can thus be modified by conjugation effects.

Finally, in (−)-**6** we cannot, even tentatively, determine the actual sign of $\theta$, in view of the extensive band cancellation occurring in the $B_{2u}$ region of the experimental CD spectrum (Figure 6).

## Conclusion

We have developed a simple theoretical model based on the Kuhn–Kirkwood exciton mechanism, for the coupling of six equivalent oscillators in a $D_3$ molecular point group. By comparing the predictions of the model with relevant experimental data, we have established its general validity and its limitations.

The model predicts for each $B_{1u}$ and $B_{2u}$ benzene transition the presence of three CD components, one ($A_2$) being polarized along the $c_3$ axis and two (E) in the plane containing the $c_2$ axis. The two E components have opposite CD signs and different intensities, the stronger having sign opposite to the $A_2$ transition. For a staggered conformation of the cryptophanes ($2\gamma = 60°$), the splittings between the two pairs of E states are estimated to be very small, compared to the corresponding $E - A_2$ energy difference, and the E components are never resolved in plotted spectra for realistic bandwidths. As a consequence, the theoretical CD curves consist, for each benzene transition, of a bisignate couplet where the $A_2$ component and the largest E component determine the sequence of signs. For an eclipsed conformation ($2\gamma = 0°$), the E states split apart, especially in the $B_{1u}$ manifold for which the splitting becomes apparent in plotted spectra, for reduced band widths. Inclusion of limited configuration interaction ($B_{2u}$–$B_{1u}$) only quantitatively modifies the theoretical description of the spectra.

We have found that the CD spectra of a series of $D_3$-cryptophanes could be, in most cases, satisfactorily interpreted in terms of this model, when the polarization directions of the transitions are set in accordance to the spectroscopic moments of the substituents by using the rules previously defined for the $C_3$-cyclotriveratrylenes. However, the two E ($B_{2u}$) components are resolved in some of the spectra, and their energy sequence is not always found in agreement with the theoretical prediction. The simplest and most probable explanation of this behavior is the failure of the point-dipole approximation to determine the sequence of energy levels of the almost degenerate pair of E components; nevertheless even in this case the sign and location of the $A_2$ component seem to be correctly predicted, and the model can still be useful. The two E ($B_{1u}$) components are unresolved in all experimental spectra; we take this result as an indirect evidence in favor of staggered conformation of the $D_3$-cryptophanes in solution.

The results of this study seem significant for several points of view: First, evidence is established for the importance of the coupled-oscillator model in explaining CD spectra of complex molecules. In addition, a uniform explanation is provided for all the molecules studied. Finally, indirect evidence about the conformation of cryptophanes in solution is obtained; so far, such information could not be obtained from other physical methods, including NMR spectroscopy.

## Experimental Section

Melting points were determined on a Kofler hot-bench apparatus. Rotations were measured on a Perkin-Elmer 241 micropolarimeter, in thermostated 1-dm quartz cells (25 °C). Circular dichroism spectra were recorded at room temperature on a Jobin-Yvon Dichrograph V instrument, in 0.01–0.5-cm quartz cells, at concentrations in the range from $6 \times 10^{-5}$ to $2.5 \times 10^{-4}$ M. Ultraviolet spectra were obtained on a Perkin-Elmer 554 spectrometer, with the same cells and solutions as for the CD measurements. Spectrometric grade dioxane, chloroform, and methanol were used for all optical measurements. $^1$H NMR spectra were recorded at 200.13 MHz on a Brucker AM200SY instrument equipped with an ASPECT 3000 computer. Mass spectra were taken on a ZAB-HF instrument, using electron impact (EI) at 70 eV, of positive fast atom bombardment ($FAB^+$) ionization techniques.

Column chromatographic filtrations and separations were carried out on Merck silica gel 60 (0.040–0.063 mm), or equivalent in other brands, or over Merck aluminum oxide 90 (0.063–0.200 mm, activity II-III). Analytical and preparative thin-layer chromatography (TLC) were performed on commercially available fluorescent (254-nm) silica gel plates (Merck, Whatman, or Mackerey-Nagel).

The syntheses of the following compounds have already been reported: **9**,[10,11] **10a**,[14] **12**,[10] and **13**.[14]

**4-(3-Iodopropoxy)-3-methoxybenzenemethanol (10b).** In a first step, the corresponding *bromide* was prepared from vanillyl alcohol (3.85 g, 0.025 mol), 1,3-dibromopropane (5 mL, 0.05 mol), and $K_2CO_3$ (3.45 g, 0.025 mol) in 5 mL of acetone. After this mixture was refluxed for 15 h, the solvent was stripped, and the residue was taken up in a mixture of water and ether, which resulted in the crystallization of the dialkylated byproduct 1,3-bis[4-(hydroxymethyl)-2-methoxyphenoxy]propane, which was separated by filtration; mp 153 °C (ethanol). Anal. Calcd for $C_{19}H_{24}O_6$: C, 65.50; H, 6.94. Found: C, 65.45; H, 7.0. The ether layer of the filtrate was washed with water, dried over $Na_2SO_4$, and filtrated through a short alumina column, and the eluate was evaporated to dryness. Yield 4.15 g (60%) of 4-(3-bromopropoxy)-3-methoxybenzenemethanol, mp 78–80 °C, which was directly converted into **10b** as follows: 3.5 g of the bromide (0.0127 mol) and 3.8 g of INa (0.025 mol) were refluxed for 8 h in 35 mL of acetone. The solvent was stripped, and the residual oil was taken up in water and extracted with ether; the crude **10b** was recrystallized from diisopropyl ether: yield 2.5 g (60%); mp 75 °C; $^1$H NMR (from $Me_4Si$ in $CDCl_3$) $\delta$ 2.32 (m, $CH_2CH_2CH_2$), 3.40 (t, $CH_2I$), 3.87 (s, $OCH_3$), 4.09 (t, $OCH_2$), 4.63 (s, $CH_2OH$), 6.90 (m, arom H). Anal. Calcd for $C_{11}H_{15}O_3I$: C, 41.01; H, 4.69. Found: C, 41.4; H, 4.8.

**4-(4-Iodo-2-butynoxy)-3-methoxybenzenemethanol (10c).** First, the corresponding *chloride* was prepared as follows. To a solution of vanillyl alcohol (3.5 g, 0.0227 mol) in 100 mL of ethanol was added 1.9 mL (0.0228 mol) of 12 N NaOH, and this mixture was heated to reflux for 10 min; then, 2.25 mL (0.0227 mol) of 1,4-dichlorobutyne was added, and the mixture was refluxed for 45 min. The solvent was evaporated, water was added, and the organic material was extracted with ether. The crude product (2.8 g) was chromatographed over 200 g of $Al_2O_3$ with use of dichloromethane/ether (1:1) as the eluant: yield 1.2 g (25%) of 4-(4-chloro-2-butynoxy)-3-methoxybenzenemethanol; mp 64–65 °C (from ether); $^1$H NMR (from $Me_4Si$ in $CDCl_3$) $\delta$ 3.89 (s, $OCH_3$), 4.15 (t, $J$ = 1.9 Hz, $CH_2Cl$), 4.64 (s, $CH_2OH$), 4.80 (t, $OCH_2$), 6.95 (m, arom H). Anal. Calcd for $C_{12}H_{13}O_3Cl$: C, 59.88; H, 5.44. Found: C, 59.7; H, 5.6. Then, this chloride (2.19 g, 0.0091 mol) and INa (3 g, 0.020 mol) were refluxed for 8 h in 35 mL of acetone. After the solvent was stripped, **10c** was crystallized from methanol/water: yield 2 g (70%); mp 75 °C (methanol); $^1$H NMR (from internal $Me_4Si$ in $CDCl_3$) $\delta$ 3.69 (t, $CH_2I$) and 4.77 (t, $OCH_2$, $J$ = 2.1 Hz), 3.89 (s, $OCH_3$), 4.64 (br d, $CH_2OH$, $J$ = 4.4 Hz), 6.83–7.02 (m, arom H). Anal. Calcd for $C_{12}H_{13}O_3I$: C, 43.39; H, 3.95. Found: C, 43.45; H, 3.98.

**2,7,12-Tris[2-[4-(hydroxymethyl)-2-methoxyphenoxy]ethoxy]-3,8,13-trimethoxy-10,15-dihydro-2*H*-tribenzo[*a*,*d*,*g*]cyclononene (*rac*- and M-(+)-11a).** *rac*-**11a** was prepared from (±)-**9**[11] (0.49 g, 1.2 mmol), in 30 mL of DMF–HMPA (1:1, v/v); 0.58 mL (3.6 mmol) of 25% aqueous NaOH was added, and the mixture was stirred under argon for 10 min, followed by addition of iodide **10a**[14] (1.11 g, 3.6 mmol). After the mixture was stirred at room temperature for 1 h, further amounts of NaOH (0.3 mL) and of **10a** (0.56 g) were added; after 1 h the reaction mixture was poured into water, and the precipitate was isolated by suction filtration and dried in air; yield 0.92 g (80%) of crude **11a** (this product may be used without further purification for the preparation of cryptophane A (1); see below). Pure **11a** was obtained by TLC on silica gel (dichloromethane/ethyl acetate/methanol, 5:4.5:0.5 (v/v) as the eluant) and recrystallization from methanol: mp ca. 105 °C (desolvation); C, H analysis, consistent with a *dihydrate*;$^1$H NMR (from internal $Me_4Si$ in $CD_3SOCD_3$) $\delta$ 3.55 (d, $H_e$) and 4.70 (d, $H_a$, $J$ = 13.5 Hz), 3.66 (s, $OCH_3$), 3.72 (s, $OCH_3$), 4.21 (br, $CH_2CH_2$), 4.39 (d, $CH_2OH$) and 5.09 (t, OH, $J$ = 5.5 Hz), 6.78 (dd, $H_\delta$), 6.90 (d, $H_{\gamma'}$, $J$ = 8 Hz) and 6.92 (d, $H_\gamma$, $J$ = 1.5 Hz), 7.08 and 7.16 (s, s, $H_{\alpha/\alpha'}$). Anal. Calcd for $C_{54}H_{60}O_{15}\cdot 2H_2O$: C, 65.84; H, 6.55. Found: C, 65.9; H, 6.4.

In the same way, 100 mg of (−)-**9**[10] having $[\alpha]_D$ −271° ($CHCl_3$) in 6 mL of DMF/HMPA was first treated with 0.12 mL of 25% aqueous NaOH and 231 mg of **10a** for 1 h at room temperature. Then the same quantities of NaOH and **10a** were added, and the reaction was allowed

to proceed to completion for 1 h more. After TLC as above and *digestion* (no heating) in methanol, 190 mg (80%) of (+)-**11a** was isolated: mp (desolvation) ca. 100 °C; $[\alpha]_D$ +73° ($CHCl_3$, *c* 0.3); same NMR and TLC behavior as the racemate.

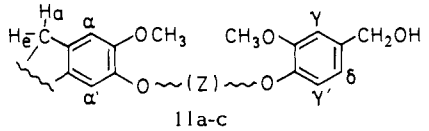

**11a-c**

**2,7,12-Tris[3-[4-(hydroxymethyl)-2-methoxyphenoxy]propoxy]-3,8,13-trimethoxy-10,15-dihydro-5*H*-tribenzo[*a*,*d*,*g*]cyclononene (*rac*- and *P*-(-)-11b).** *rac*-**11b** was prepared from (±)-**9**[11] (408 mg, 1 mmol), 25% aqueous NaOH (0.5 mL, then 0.125 mL), and iodide **10b** (1 g, then 0.25 g) in 20 mL of DMF/HMPA exactly as described above for the preparation of **11a**. The crude **11b** was then chromatographed over 100 g of silica gel with use of a dichloromethane/acetone mixture (7:3, v/v) as the eluant: yield 350 mg (36%) of an amorphous powder, which was used without further purification for the next step; $^1H$ NMR (from internal $Me_4Si$ in $CDCl_3$) $\delta$ 2.29 (m, $CH_2CH_2CH_2$), 3.51 (d, $H_e$) and 4.73 (d, $H_a$, $J$ = 13.8 Hz), 3.70 (s, $OCH_3$), 3.77 (s, $OCH_3$), 4.17 (m, $OCH_2CH_2CH_2$), 4.57 (s, $CH_2OH$), 6.78 (dd, $H_\delta$), 6.82 (d, $H_{\gamma'}$, $J$ = 8 Hz) and 6.86 (d, $H_\gamma$, $J$ = 1.5 Hz), 6.82 and 6.91 (s, s, $H_{\alpha/\alpha'}$).

Similarly, 41 mg (0.1 mmol) of (+)-**9**[10] having $[\alpha]_D$ +271° ($CHCl_3$) gave P-(-)-**11b** (80 mg), $[\alpha]_D$ -43° ($CHCl_3$, *c* 0.3), whose $^1H$ NMR spectrum and TLC behavior were identical with those of the racemate.

**2,7,12-Tris[4-[4-(hydroxymethyl)-2-methoxyphenoxy]-2-butynoxy]-3,8,13-trimethoxy-10,15-dihydro-5*H*-tribenzo[*a*,*d*,*g*]cyclononene (*rac*- and P-(-)-11c).** The cyclization precursor **11c** can be prepared from either the iodide **10c** or the corresponding *chloride* (lower yield). We describe here the synthesis of *rac*-**11c** from the *chloride* and that of (-)-**11c** from the *iodide*.

Thus, *rac*-**11c** was prepared from (±)-**9**[11] (209 mg, 0.5 mmol), 25% aqueous NaOH (0.26 mL, then 0.13 mL), and the chloride analogue of **10c** (360 mg, then 180 mg) in 10 mL of DMF/HMPA as described above for the preparation of **11a**, except for the isolation procedure: Water was added, and the organic material was extracted with ethyl acetate; the organic layer was washed with water and dried, and the solvent was evaporated off. The crude **11c** was chromatographed over a silica gel column with use of dichloromethane/ether (8:2) and then dichloromethane/methanol (98:2, v/v) as the eluants; yield 275 mg (55%) of **11c** (glass), which was used without further purification for the next step; $^1H$ NMR (from internal $Me_4Si$ in $CDCl_3$) $\delta$ 3.60 (d, $H_e$) and 4.76 (d, $H_a$, $J$ = 13.7 Hz), 3.76 (s, $OCH_3$), 3.84 (s, $OCH_3$), 4.57 (s, $CH_2OH$), 4.69 (m, $CH_2C{\equiv}CCH_2$), 6.68 (dd, $H_\delta$), 6.79 (d, $H_\gamma$, $J$ = 8.1 Hz) and 6.89 (d, $H_{\gamma'}$, $J$ = 1.8 Hz), 6.76 and 6.91 (s, s, $H_{\alpha/\alpha'}$).

For the preparation of *P*-(-)-**11c**, 41 mg (0.1 mmol) of (+)-**9**[10] having $[\alpha]_D$ +271° ($CHCl_3$) in 3 mL of DMF/HMPA was first treated with 0.05 mL (0.3 mmol) of 25% aqueous NaOH and 100 mg (0.3 mmol) of the iodide **10c** (1 h at 0 °C); further amounts of NaOH (0.025 mL) and of **10c** (50 mg) were then added, and the mixture was stirred at room temperature for 2 h. Water was added, and the pasty precipitate was separated and triturated with cold methanol: yield 105 mg (100%) of (-)-**11c**, which was used without further purification; $[\alpha]_D$ -66° ($CHCl_3$, *c* 0.34); $^1H$ NMR, spectrum identical with that of the racemate.

**Cryptophane A ((*rac*- and (-)-1).** Because **1** is easier to purify than the sparingly soluble precursor **11a**, it may be convenient to use crude **11a** as the starting material for the cyclization. Several typical procedures for the preparation of **1** from either crude or purified **11a** are described here.

***rac*-1.** (I) in a 250-mL rotatory evaporator flask was dissolved 75 mg of purified (±)-**11a** in 75 mL of formic acid (concentration $1 \times 10^{-3}$ M); the flask was fitted to the evaporator and heated in the water bath at 55-60 °C for 3 h, with slow rotation. The solvent was stripped under reduced pressure (some $CHCl_3$ was added at the end in order to facilitate formic acid removal through azeotrope formation), and the cryptophane was isolated by TLC on silica gel with use of dichloromethane/methanol (95:5, v/v) as the eluant; a glass was obtained (56 mg, 80%), which crystallized in the presence of methanol; 52 mg of pure **1** (NMR, TLC) was isolated in this way. (II) 435 mg of *crude* **11a** in 435 mL of formic acid was similarly treated (3 h, 55-60 °C), giving after TLC 273 mg (66%) of nearly pure **1**; after crystallization in methanol, 155 mg (40%) of pure material was obtained. (III) When the same reaction, from crude **11a**, was effected at 90 °C, the yield of **1** after TLC was 47%. (IV) For the same reaction at room temperature for 48 h, the yield after TLC was 53%. (V) A solution of crude **11a** (40 mg) in 10 mL of glacial acetic acid was placed in a dropping funnel fitted with a capillary glass tube and was slowly added (5 h) to a magnetically stirred mixture of acetic acid (30 mL) and 65% perchloric acid (10 mL), at room temperature. Then, water was added, and the organic material was extracted with dichloromethane; the organic layer was washed with aqueous NaOH (*Caution*! All the perchloric acid must be removed at this step.) and with water until neutral, dried, and evaporated to dryness. After TLC as above, 12 mg (30%) of **1** was obtained.

A sample of (±)-**1** recrystallized from dioxane/methanol was satisfactorily analyzed for a *dihydrate*. Anal. Calcd for $C_{54}H_{54}O_{12}\cdot 2H_2O$: C, 69.66; H, 6.28. Found: C, 69.5; H, 6.1. A sample crystallized from $CHCl_3$ was nearly exactly analyzed for $C_{54}H_{54}O_{12}\cdot CHCl_3$. Anal. Calcd: C, 65.12; H, 5.47. Found: C, 64.7; H, 6.0. EI mass spectrum, $M^+$ m/z 804, $M^{2+}$ m/z 447; $^1H$ NMR (from $Me_4Si$ in $CDCl_3$) $\delta$ 3.41 (d, $H_e$) and 4.60 (d, $H_a$, $J$ = 13.8 Hz), 3.80 (s, $OCH_3$), 4.17 (br s, $OCH_2CH_2O$), 6.67 and 6.76 (s, s, arom H).

(-)-1. The following procedures were used. (VI) A solution of (+)-**11a** (having $[\alpha]_D$ +74° in $CHCl_3$) in 10 mL of formic acid was added dropwise (20 min) to 40 mL of magnetically stirred formic acid at 85 °C. After TLC (same eluant as for the racemate) and digestion in methanol containing a small amount of dichloromethane, 15 mg (40%) of (-)-**1** was isolated, having $[\alpha]_D$ -211° ($CHCl_3$, *c* 0.18); after a second TLC, followed by digestion in acetone, (-)-1 showed $[\alpha]_D$ -230° ($CHCl_3$, *c* 0.26). (VI) A solution of (+)-**11a** (50 mg) in 50 mL of acetic acid was added in 5 h to 10 mL of 65% perchloric acid (magnetically stirred) at room temperature. The isolation procedure was the same as in (V) above. After TLC and digestion in methanol, 15 mg (32%) of (-)-**1** were obtained, $[\alpha]_D$ -254° ($CHCl_3$, *c* 0.18). (VII) The same conditions as in (VI) were used except that the acetic acid solution and the perchloric acid were placed in two dropping funnels and simultaneously added into the flask during the course of 5 h: yield 35%; $[\alpha]_D$ -239° ($CHCl_3$, *c* 0.17). (VIII) A 35-mg portion of (+)-**11a** in 70 mL of formic acid, heated for 4 h at 55 °C, afforded 23 mg (70%) of (+)-**1**, $[\alpha]_D$ -237° ($CHCl_3$, *c* 0.26). (IX) A 140-mg portion of (+)-**11a** in 280 mL of formic acid, heated for 4 h at 55 °C, yielded 95 mg (72%) of (-)-**1** with $[\alpha]_D$ -231° ($CHCl_3$, *c* 0.3).

The NMR and TLC behavior of (-)-**1** were identical with those of the racemate.

**Cryptophane E (*rac*- and (+)-2) and Cryptophane F (*meso*-7).** *rac*-**2** and *meso*-**7** were prepared as follows. In a 1-L rotatory evaporator flask was dissolved (±)-**11b** (300 mg, 0.31 mmol) in 3 mL of $CHCl_3$, and 600 mL of formic acid was then added (concentration $5.2 \times 10^{-4}$ M). The flask was fitted to the evaporator and heated in the water bath at 60 °C for 3 h, with slow rotation. The solvent was evaporated under vacuum (some $CHCl_3$ was added at the end in order to facilitate formic acid removal through azeotrope formation). The resulting solid was dissolved in 150 mL of $CHCl_3$, and the solution was loaded onto a column containing 100 g of silica gel. On elution with a chloroform/acetone mixture (9:1, v/v), 137 mg of crude (±)-**2** was isolated; next, 185 mg of meso isomer **7** was recovered by elution with chloroform/methanol (95:5, v:v). *rac*-**2** was purified by TLC on silica gel (dichloromethane/acetone, 9:1, $R_f$ 0.47): yield 77 mg (27%); no mp (>260 °C); EI mass spectrum, $M^+$ *m/z* 937; $^1H$ NMR (from internal $Me_4Si$ in $CDCl_3$) $\delta$ 2.32 (br s, $CH_2CH_2CH_2$), 3.43 (d, $H_e$) and 4.66 (d, $H_a$, $J$ = 13.5 Hz), 3.83 (s, $OCH_3$), 3.98 (m, $OCH_2$), 6.61 and 6.69 (s, s, arom H's). *meso*-**7**, which was sparingly soluble in all usual solvents, was purified by digestion in $CHCl_3$: yield 150 mg (50%); EI and $FAB^+$ mass spectra, $M^+$ *m/z* 937; $^1H$ NMR (in $C_2D_2Cl_2$, with $C_2DHCl_2$ 5.99) $\delta$ 1.9 (m, $CH_2CH_2CH_2$), 3.37 (d, $H_e$), 4.53 (d, $H_a$, $J$ = 13 Hz), 3.66 (s, $OCH_3$), 3.77 (m, $OCH_2$), 6.60 and 6.66 (s, s, arom H).

For the preparation of (+)-**2**, 63 mg of (-)-**11b** was dissolved in 150 mL of formic acid in a 500-mL rotatory evaporator flask, and this solution was heated in a water bath (90 °C) for 1 h. After the solvent was stripped under vacuum (with addition of $CHCl_3$ at the end), the two isomeric cryptophanes (+)-**2** and **7** were separated by TLC (dichloromethane/acetone, 9:1); 10 mg (16%) of the faster running (+)-**2** ($R_f$ 0.47) was obtained, with $[\alpha]_D$ +49° ($CHCl_3$, *c* 0.9; see Table I) and NMR identical with that of the above racemate; the slower running isomer (25 mg, 40%, $R_f$ 0.05) showed no rotation and in all respects was identical with the above sample of **7**.

**Cryptophane G (*rac*- and (+)-3) and Cryptophane F (*meso*-8).** *rac*-**3** and *meso*-**8**: 270 mg of (±)-**11c** in 3 mL of $CHCl_3$ was added to 550 mL of formic acid, in a 1-L rotatory evaporator flask; this solution was heated at 60 °C for 3 h, and formic acid was stripped as described for the preparation of **2** above. The crude cryptophane mixture was separated by TLC, using chloroform/ether (85:15, v/v) as the eluant; 110 mg (43%) of the faster running (±)-**3** and 51 mg (20%) of the slower running **8** were obtained; after digestion in methanol, both compounds had mp >260 °C and in $FAB^+$ mass spectra showed $M^+$ *m/z* 967. $^1H$ NMR (from internal $Me_4Si$ in $CDCl_3$): cryptophane G ((±)-**3**), $\delta$ 3.44 (d, $H_e$) and 4.64 (d, $H_a$, $J$ = 13.5 Hz), 3.84 (s, $OCH_3$), 4.51 (d) and 4.83 (d, $OCH_2C{\equiv}CCH_2O$, $J$ = 16 Hz), 6.75 and 6.82 (s, s, arom H's); cryptophane H (**8**), $\delta$ 3.46 (d, $H_e$) and 4.64 (d, $H_a$, $J$ = 13.5 Hz), 3.78 (s, $OCH_3$), 4.31 (dd), and 4.94 (dd, $OCH_2CCCH_2O$, $J$ = 16 Hz and 1

Hz), 6.74 and 6.80 (s, s, arom H's).

Optically active cryptophane G ((+)-**3**) was similarly prepared from 100 mg of (-)-**11c** in 2 mL of $CHCl_3$ and 200 mL of formic acid for 1 h at 90 °C. TLC separation as above gave 35 mg of (+)-**3**, $[\alpha]_D$ +199° ($CHCl_3$, *c* 0.43), and 22 mg of **8** (showing no rotation). (+)-**3** was recrystallized from methanol: yield 28 mg, 30%; $[\alpha]_D$ +201° ($CHCl_3$, *c* 0.44; see Tables I and II). **8** was recrystallized from acetone; yield 13 mg, 14%. $^1H$ NMR spectra of (+)-**3** and **8** were identical with those of *rac*-**3** and *meso*-**8** given above.

**Cryptophanol A (*rac*- and (-)-4).** ***rac*-4**: To 225 mg (0.25 mmol) of *rac*-**1** was added 3 mL of a 1 M THF solution of lithium diphenylphosphide,[21b] and the resulting deep red mixture was stirred at room temperature for 24 h under argon atmosphere. Water was added, and some neutral material was extracted with ether. On acidification (concentrated HCl), the aqueous phase afforded a white precipitate of **4**, which was collected by suction filtration, washed with water, and then digested in refluxing THF: yield 125 mg (60%); mp >260 °C; C, H analysis, consistent with a *trihydrate*; $^1H$ NMR (from $Me_4Si$ in $CD_3COCD_3$) $\delta$ 3.16 (d, $H_e$) and 4.40 (d, $H_a$, $J$ = 13.5 Hz), 4.40 (s, $OCH_2$), 6.63 and 6.73 (s, s, arom H), 7.7 (OH). Anal. Calcd for $C_{48}H_{42}O_{12}\cdot 3H_2O$: C, 66.66; H, 5.59. Found: C, 67.0; H, 5.3.

(-)-**4**: The (-) enantiomer of **4** was similarly prepared from 50 mg of (-)-**1** (0.056 mmol) having $[\alpha]_D$ -231° ($CHCl_3$) and 1.5 mL of 1 M lithium diphenylphosphide in THF. For the CD measurements, a sample was recrystallized from THF: $[\alpha]_D$ -172° (DMF, *c* 0.21; see Tables I and II); analytical TLC behavior of (-)-**4**, identical with that of the racemate (dichloromethane/methanol, 95:5 (v/v)).

**Cryptophanol A Hexaacetate ((-)-5).** This compound was prepared by reaction of (-)-**4** (12 mg) and acetic anhydride (0.5 mL) in 1 mL of pyridine for 1 h at room temperature. The solution was poured into water, and the precipitate of (-)-**5** was collected by suction filtration and was finally purified by TLC (dichloromethane/acetone, 9:1 (v/v)) and by digestion in ether: yield 9 mg of a solid (mp >260 °C); $[\alpha]_D$ -24° ($CHCl_3$, *c* 0.24; see Tables I and II); $^1H$ NMR (from internal $Me_4Si$ in $CDCl_3$) $\delta$ 2.35 (s, $OCOCH_3$), 3.48 (d, $H_e$) and 4.58 (d, $H_a$, $J$ = 13.7 Hz), 3.80-4.35 (m, $OCH_2CH_2O$), 6.86 and 6.92 (s, s, arom H).

**Cryptophanol A, Hexakis[*O*-(carbomethoxy)methyl] (*rac*- and (-)-6).** To *rac*-**4** (50 mg, 0.0617 mmol) in DMF (2 mL) was added 125 mg (0.38 mmol) of $Cs_2CO_3$; after 1 h stirring at room temperature, 0.075 mL (ca, 2 equiv) of methyl bromoacetate was added, and the mixture was heated for 20 h at 60 °C under nitrogen. Water was added, and the precipitate was collected by suction filtration, washed with methanol, and then recrystallized from chloroform-methanol: yield 50 mg (65%); mp ca. 195 °C; $FAB^+$ mass spectrum, $M^+$ *m/z* 1243.54 (calcd 1243.27); C,H analysis, consistent with a *tetrahydrate*. $^1H$ NMR (from $Me_4Si$ in $CD_3COCD_3$) $\delta$ 3.34 (d, $H_e$) and 4.55 (d, $H_a$, $J$ = 13.6 Hz), 3.82 (s, $COOCH_3$), 4.41 (m, $OCH_2CH_2O$), 4.66 and 4.77 (AB q, $OCH_2CO_2$ (diastereotopic H, $J$ = 15.9 Hz)), 6.82 and 6.89 (s, s, arom H). Anal. Calcd for $C_{66}H_{66}O_{24}\cdot 4H_2O$: C, 60.27; H, 5.67. Found: C, 60.04; H, 5.3.

Similarly, 37 mg of (-)-**4**, 100 mg of $Cs_2CO_3$, and 0.075 mL of methyl bromoacetate in 1.5 mL of DMF gave 28 mg (53%) of (-)-**6**, after TLC and recrystallization from chloroform/methanol: $[\alpha]_D$ -116° ($CHCl_3$, *c* 0.39; see Tables I and II); analytical TLC and $^1H$ NMR, identical with that of the racemate.

# Chemical vs. Redox Catalysis of Electrochemical Reactions. Reduction of *trans*-1,2-Dibromocyclohexane by Electrogenerated Aromatic Anion Radicals and Low Oxidation State Metalloporphyrins

**Doris Lexa, Jean-Michel Savéant,* Khac Binh Su, and Dan Li Wang**

*Contribution from the Laboratoire d'Electrochimie Moléculaire de l'Université de Paris 7, Unité Associée au CNRS N°438, 2 place Jussieu, 75251 Paris Cedex 05, France.*
*Received February 13, 1987*

**Abstract:** Homogeneous catalysis of the electrochemical reduction of *trans*-1,2-dibromocyclohexane is investigated in a series of catalysts comprising aromatic and heteroaromatic compounds and several metalloporphyrins. The aromatic anion radicals and the reduced Zn and Cu porphyrins give rise to a typical redox catalysis involving an outer-sphere electron transfer from the mediator to the substrate. The rate-determining step of the reaction as well as that of the direct electrochemical reduction at glassy carbon consists of the injection of one electron concerted with the cleavage of one carbon–bromine bond. The final olefin is obtained in successive steps after injection of a second electron and cleavage of a second bromide ion. The direct reduction and the redox-catalyzed reaction follow the same quadratic activation driving force free energy relationship involving two additive reorganization factors. One, accounting for about 80% of the standard activation energy, concerns the breaking of the C–Br bond giving a contribution approximately equal to one-fourth of the bond dissociation energy. The remainder of the activation barrier involves solvent reorganization. Nickel, iron, and cobalt porphyrins (at the formal metal "I" oxidation state) react much more rapidly than redox catalysts having the same standard potential. This points to an inner-sphere mechanism: abstraction of one Br followed by or concerted with the elimination of the second Br or $S_N2$ displacement of one $Br^-$ followed by or concerted with the elimination of the second $Br^-$ before or after the injection of a second electron.

Very numerous electrochemical reactions require a significant overpotential to proceed at appreciable rates owing to the slowness and irreversibility of the electron transfer and/or chemical steps they involve. Homogeneous catalysis of such electrochemical processes may be carried out along two conceptually different types of mechanisms.[1] In one case, "redox catalysis",[1] the active form of the catalyst, generated at the electrode, exchanges electrons with the reactant in an outer-sphere manner yielding the reaction products and regenerating the starting form of the catalyst. Catalysis[2] then results from physical rather than chemical reasons: the possibility of diminishing the overpotential is a consequence of the three-dimensional dispersion of the electron-transfering agent as opposed to the two-dimensional availability of the

(1) Andrieux, C. P.; Dumas-Bouchiat, J. M.; Savéant, J. M. *J. Electroanal. Chem.* **1978**, *87*, 39.

(2) In both cases the efficiency of the catalysis is referred to an outer-sphere electrode process in which there is no surface catalysis of the reaction by the electrode material.

0002-7863/87/1509-6464$01.50/0 